DOI: 10.1002/chem.200600220

Probing the Lewis Acidity and Catalytic Activity of the Metal–Organic Framework $[Cu_3(btc)_2]$ (BTC = Benzene-1,3,5-tricarboxylate)

Luc Alaerts,[a] Etienne Séguin,[b] Hilde Poelman,[c] Frédéric Thibault-Starzyk,[b] Pierre A. Jacobs,[a] and Dirk E. De Vos*[a]

Abstract: An optimized procedure was designed for the preparation of the microporous metal–organic framework (MOF) $[Cu_3(btc)_2]$ (BTC = benzene-1,3,5-tricarboxylate). The crystalline material was characterized by X-ray diffraction, optical microscopy, SEM, X-ray photoelectron spectroscopy, N_2 sorption, thermogravimetry, and IR spectroscopy of adsorbed CO. CO adsorbs on a small number of Cu_2O impurities, and particularly on the free Cu^{II} coordination sites in the framework. $[Cu_3(btc)_2]$ is a highly selective Lewis acid catalyst for the isomerization of terpene derivatives, such as the rearrangement of α-pinene oxide to campholenic aldehyde and the cyclization of citronellal to isopulegol. By using the ethylene ketal of 2-bromopropiophenone as a test substrate, it was demonstrated that the active sites in $[Cu_3(btc)_2]$ are hard Lewis acids. Catalyst stability, re-usability, and heterogeneity are critically assessed.

Keywords: carbon monoxide · heterogeneous catalysis · IR spectroscopy · Lewis acids · metal–organic frameworks

Introduction

Metal–organic frameworks (MOFs) are an emerging class of crystalline porous materials. They are mostly constructed from clusters of transition-metal ions held in position in a lattice by ligation to organic molecules. The free space between the metal clusters and ligands shows up as pores in the eventual structure.[1–4] In literature, the term MOF covers a wide assembly of hybrid compounds.[4,5] Because of the exceptionally high pore volume and surface area of MOFs, many research efforts have been spent to their application in the sorption of light gases, either as such[6–10] or after modification with, for example, Ba^{2+}.[11] As porous materials, MOFs may also find applications in catalysis.[12–14] The pores of MOFs can theoretically be tailored in a systematic way and hence optimized to a specific catalytic application.[3,9] Besides the high metal content of MOFs, one of their greatest advantages is that all active sites are identical, because of the highly crystalline nature of the material.[3,13,14] However, other elements might hamper application of MOFs in catalysis. As MOFs are synthesized under relatively mild conditions of temperature and pressure, they are mostly not stable beyond 600 K.[13] Moreover, some MOFs seem unstable towards water in solvent concentrations, or even to atmospheric moisture.[15–17] The stability of MOFs in other solvents should be assessed as well, as should leaching of metal ions or organic ligands.[5] For optimal catalytic activity, the active sites should be freely accessible to reagent molecules, preferably via large channels or cavities.[13] However, in many MOFs the metal ions are integral parts of the framework, and therefore they are completely saturated by coordination to the organic ligands.[4,18,19] For all these reasons, reports on the catalytic activity of MOFs are extremely scarce, and even for the best known structures, there is little understanding of the catalytic activity or applicability.

This study aims to characterize in a systematic way the acid character of $[Cu_3(btc)_2]$ (BTC = benzene-1,3,5-tricarboxylate). $[Cu_3(btc)_2]$ is a rigid MOF with a zeolite-like structure and with free coordination sites on the Cu^{II} ion. It contains three types of pores, of which the larger two penetrate the structure in all three dimensions and are connected with pore windows of ca. 6 Å in diameter. The free coordi-

[a] L. Alaerts, Prof. Dr. P. A. Jacobs, Prof. Dr. D. E. De Vos
Centre for Surface Chemistry and Catalysis
K.U.Leuven, Kasteelpark Arenberg 23, 3001 Heverlee (Belgium)
Fax: (+32) 16-321-998
E-mail: dirk.devos@biw.kuleuven.be

[b] E. Séguin, Dr. F. Thibault-Starzyk
Laboratoire Catalyse & Spectrochimie
CNRS-UMR 6506, ENSICAEN, Boulevard Maréchal Juin 6
14050 Caen CEDEX (France)

[c] Dr. H. Poelman
Department of Solid State Sciences
Ghent University, Krijgslaan 281 S1, 9000 Gent (Belgium)

nation sites are oriented towards the center of one of the larger pore types.[2,13,20] In one previous report on the catalytic activity of $[Cu_3(btc)_2]$, the material has been demonstrated to act as a Lewis acid in cyanosilylation of aldehydes.[13] At present, it is unclear whether this material can be used in other acid-catalyzed reactions. Additionally, not only Lewis acid Cu^{II} ions, but also the Brønsted carboxylic acids may contribute to the acidity. As the structure contains large amounts of carboxylates, some of these might indeed be protonated and thus contribute to the catalytic activity. Therefore, the approach of the present paper is to use specific catalytic test reactions in which the product distribution is dependent on the acid properties of the catalyst. As an alternative way to examine acidity, adsorbed probe molecules are studied by IR spectroscopy.[21]

Results

Characterization: The MOF $[Cu_3(btc)_2]$ was prepared using different synthesis methods, described in the Experimental section and summarized in Table 1. As **Cu1a** proved to be our best catalyst, most characterization techniques were applied to these samples. Images of $[Cu_3(btc)_2]$ obtained with light microscopy and SEM show the clear octahedral shape of $[Cu_3(btc)_2]$ crystals (Figures 1 and 2, respectively). Catalysts **Cu1a–f** had an average crystal size of about 20 μm; crystals of **Cu3** were somewhat smaller. Much larger crystals of about 100 μm were obtained for **Cu2**. With both light microscopy and SEM, a second, platelet-like crystal type is sporadically observed, with a shape best described as that of a sliced octahedron. Moreover, the presence of very small quantities of Cu_2O as red spheres of approximately 20 μm in diameter is revealed. X-ray diffraction patterns of different $[Cu_3(btc)_2]$ samples are shown in Figure 3; these are all in complete accordance with literature data.[13] No significant differences were noticed between the samples and none of the impurities previously mentioned were observable. Small variations in intensities can be ascribed to a different degree of hydration.[13] With nitrogen physisorption measurements specific surfaces between 1200 and 1400 $m^2 g^{-1}$ and pore volumes between 0.60 and 0.65 $cm^3 g^{-1}$ were measured for different **Cu1a** and **Cu2** batches. The values obtained are higher than those reported in literature.[2,7,13] All sorption curves were of type I and no hysteresis loop was noticed.

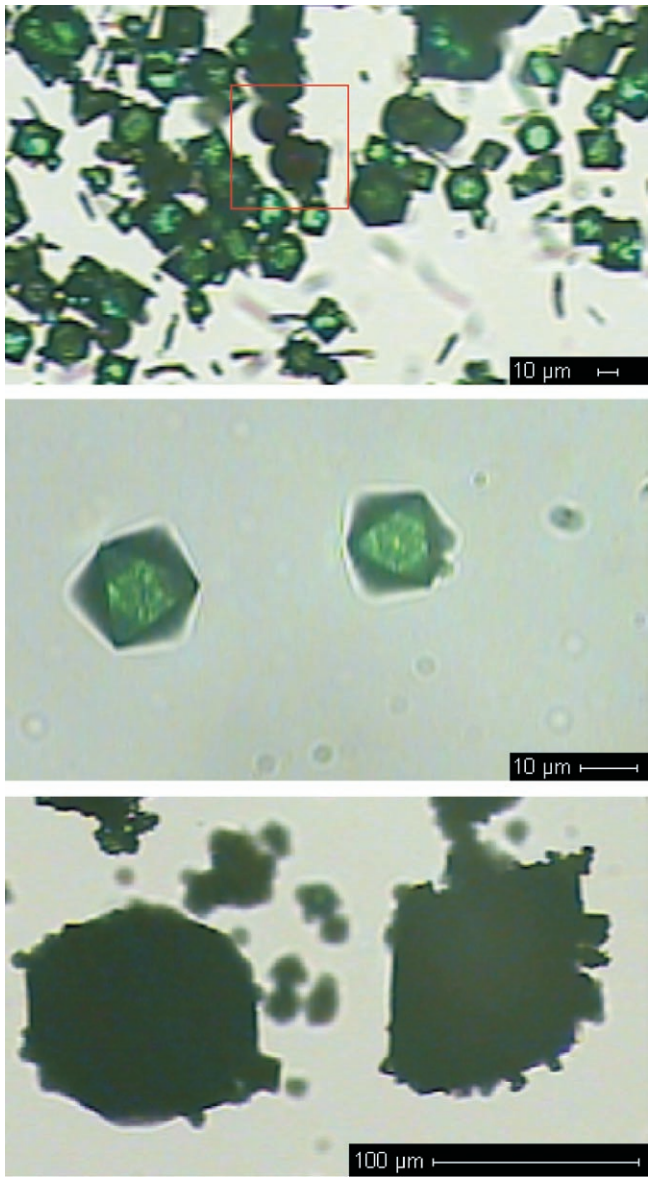

Figure 1. Images of freshly prepared crystals of $[Cu_3(btc)_2]$. Top: Octahedral crystals of **Cu1a**. Dark red spherical Cu_2O particles are visible inside the red square. Middle: zoom on **Cu1a** octahedra. Bottom: Very large crystals of **Cu2**.

The adsorption and desorption curve of **Cu1a** is shown in Figure 4. The thermal stability of **Cu1a** was studied in a

Table 1. Overview of different synthesis procedures for $[Cu_3(btc)_2]$.

	Ref.	Modifications	Washing and drying treatments[a]
Cu1a	[13]	383 K, 15 h	2×water:ethanol (50:50); 3×doubly distilled water
Cu1b	[13]	383 K, 15 h	3×water, quickly
Cu1c	[13]	383 K, 15 h	3×water, thoroughly
Cu1d	[13]	383 K, 15 h	3×ethanol
Cu1e	[13]	383 K, 15 h	3×water/ethanol (50:50)
Cu1f	[13]	383 K, 15 h	2×water/ethanol (50:50); 3×doubly distilled water; 4 h at 333 K, 15 h at 473 K
Cu2	[7]	383 K, 15 h	2×water/ethanol (50:50); 3×doubly distilled water
Cu3	[13]	383 K, 15 h; half of described concentration	2×water/ethanol (50:50); 3×doubly distilled water

[a] Unless mentioned otherwise, samples were dried for 4 h at 333 K and next for 15 h at 383 K.

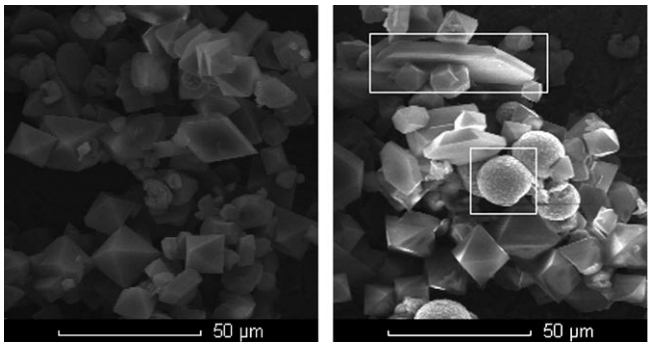

Figure 2. Images of freshly prepared crystals of **Cu1a** obtained by SEM. Left: Well-shaped octahedra. Right: Focus on spherical Cu_2O particles (square) and platelet-like crystals (rectangle).

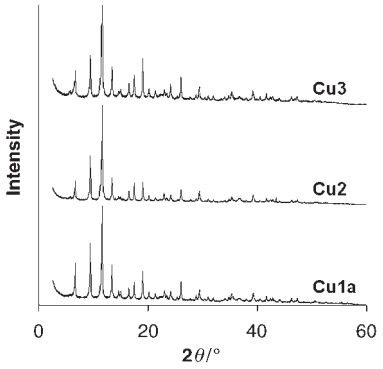

Figure 3. X-ray diffractograms of $[Cu_3(btc)_2]$ obtained with different synthesis procedures.

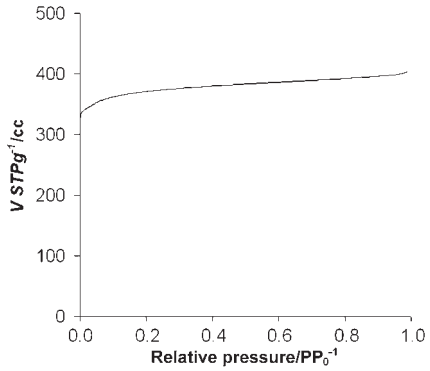

Figure 4. Nitrogen adsorption isotherm of **Cu1a**. Desorption and adsorption curves coincide.

thermogravimetric analysis (TGA) experiment (Figure 5). Loss of physisorbed water gives rise to the first step in the curve. The exact height of this step depends on the initial degree of hydration of the catalyst. After a plateau, a second step indicates the disintegration of the metal–organic structure from 550 K on. Similar TGA curves are obtained for the other $[Cu_3(btc)_2]$ samples. A simulation of the drying procedure is shown in Figure 6. It seems that no water is left in the structure after "overnight drying" at 373 K because of the absence of a second weight-loss step. The outer surface

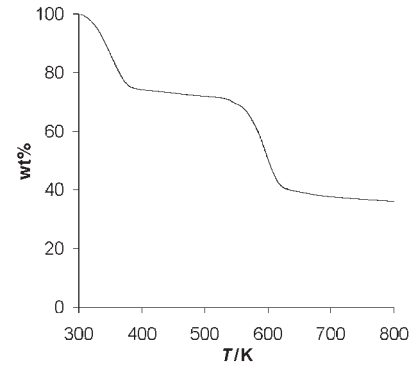

Figure 5. Weight loss in function of temperature for $[Cu_3(btc)_2]$ upon heating (5 K min^{-1}) in N_2.

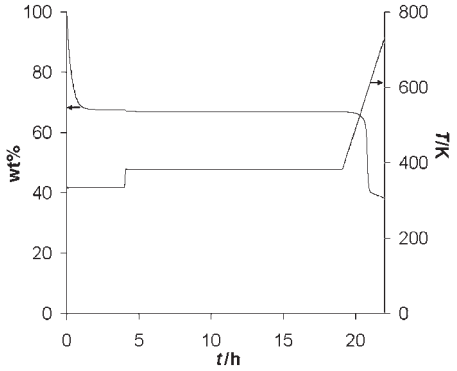

Figure 6. Weight loss and temperature versus time for $[Cu_3(btc)_2]$ in a simulation of the drying procedure: 4 h at 333 K, then 15 h at 383 K.

of the catalyst particles was examined by X-ray photoelectron spectroscopy. The main Cu 2p3/2 peak of divalent Cu^{2+} is observed at 933 eV; contributions of other Cu species were not sufficient to be resolved from the main peak. The C1s photoemission line was clearly composed of two contributions: the 284.6 eV binding energy corresponds to the carbon atoms in the aromatic ring, while the 288.5 eV signal arises from the carboxyl groups. Their respective contribution to the overall C1s signal was determined through curve fitting. Atomic percentages of the surface atoms of $[Cu_3(btc)_2]$ are given in Table 2, together with their stoichiometric percentages. Clearly, the composition of the surface is not significantly different from that of the bulk structure. No supplementary oxygen signals of protonated carboxylic groups were seen. In summary, none of the phase impurities observed by light or electron microscopy could be detected by other bulk or surface analysis techniques.

Table 2. Atomic percentages of Cu, C, and O on the surface of $[Cu_3(btc)_2]$ as measured by XPS.

	Cu	C, aromatic	C, carboxylate	O
measured atom %	9.8	35.9	17.2	37.1
calculated atom %	9.1	36.4	18.2	36.4

Isomerization of α-pinene oxide: A first catalytic test reaction for acidity is the isomerization of α-pinene oxide (**1**) to campholenic aldehyde (**2**), shown in Scheme 1. Compound **2**

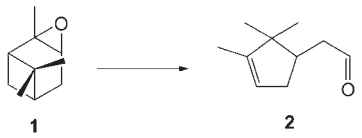

Scheme 1. Isomerization of α-pinene oxide (**1**) to campholenic aldehyde (**2**).

is an important fragrance compound; it can only be prepared in high yield when a suitable Lewis acid is used. Metal halogenides seem to be the best homogeneous catalysts for this reaction, but the search for heterogeneous catalysts is still of current interest.[22] Brønsted acids tend to produce, besides **2**, a mixture of compounds in low yields, like *trans*-carveol, *p*-cymene, *trans*-sobrerol, and dimerization products. The selectivity to **2** is usually not higher than 55% with Brønsted acids, while with Lewis acids selectivities as high as 85% can be reached.[21,23,24] As **1** is highly reactive, reactions were performed at room temperature. As only compound **2** is of interest, yields of other products are not reported here. First, reactions were carried out with different $[Cu_3(btc)_2]$ samples in several solvents. The obtained selectivities of **2** are given in Table 3. All reported selectivities

Table 3. Selectivities [%] of **2** obtained with different $[Cu_3(btc)_2]$ catalysts. Reactions were carried out at room temperature with for each reaction 0.1 g of α-pinene oxide in 5 mL of solvent added to 0.1 g of $[Cu_3(btc)_2]$.[a]

	DCE	EtOAc	MeOH	CH_3CN	Toluene
Cu1a	84	80	66	86	67
Cu1b	83	81	68	n.d.	n.d.
Cu1c	83	75	54	n.d.	n.d.
Cu1d	83	72	70	n.d.	n.d.
Cu1e	83	76	76	n.d.	n.d.
Cu1f	79	n.d.	n.d.	n.d.	n.d.
Cu2	83	84	63	n.d.	n.d.
Cu3	85	n.d.	n.d.	n.d.	n.d.

[a] DCE = 1,2-dichloroethane; n.d. = not determined; selectivities remained constant till complete conversion.

were reproducible within 2% and were constant until complete conversion. For reactions in methanol, no methanolysis of **1** was detected.

Regarding the selectivity of the reaction, 1,2-dichloroethane (DCE) seems most suitable of all tested solvents. The overall selectivities are above 80%, except for **Cu1f**, which shows that drying at a higher temperature does not improve the selectivity. A high selectivity is also reached in acetonitrile. No influence of the washing procedure was noted for reactions in DCE; however, this is not the case for the reactions carried out in ethyl acetate or methanol. A comparison between the catalytic properties of $[Cu_3(btc)_2]$ obtained by means of different synthesis procedures (**Cu2** and **Cu3**) was only carried out in DCE. No significant change of the selectivity was seen.

The conversion of **1** as a function of time in different solvents with **Cu1a** is given in Figure 7. The highest reaction

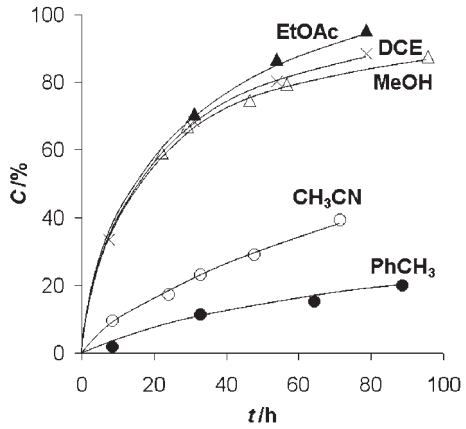

Figure 7. Conversion of **1** versus time with **Cu1a** in different solvents.

rate was obtained in ethyl acetate as solvent, followed by DCE and methanol. The reaction proceeds very slowly in acetonitrile and toluene. The effect of different pretreatments and synthesis procedures of $[Cu_3(btc)_2]$ on reaction rates is shown in Figure 8. Reaction rates in methanol are

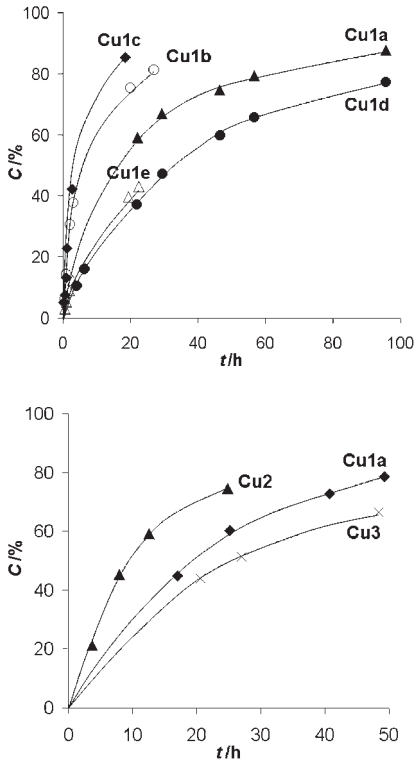

Figure 8. Conversion of α-pinene oxide over $[Cu_3(btc)_2]$ as a function of time. Top: different catalyst pretreatments; reaction solvent = MeOH. Bottom: different synthesis procedures; reaction solvent = 1,2-dichloroethane.

heavily influenced by the solvent pretreatment of $[Cu_3(btc)_2]$ (Figure 8, top). With catalyst samples that were thoroughly washed in pure water (**Cu1c**), the obtained reaction rate was highest, followed by the samples quickly washed in water (**Cu1b**). Washing in ethanol (**Cu1d**) had a negative effect on the reaction rate, as is the case for washing with an ethanol/water 50:50 mixture (**Cu1e**). Successive washing in ethanol and water (**Cu1a**) resulted in an intermediate reaction rate. This suggests that residual ethanol, not detectable by TGA, may still reside within the structure and partially block some of the active sites. On the other hand, solvent washing might affect the microporosity during drying.[7] For reactions in DCE, different washing procedures, or different synthesis methods and ensuing crystal sizes did not result in large variations in reaction rate (Figure 8, bottom). Since the largest rates were observed for the largest crystals, it is improbable that the reaction is hindered by internal diffusion limitation. For the reactions in DCE, the activation energy was estimated at 95 kJ mol^{-1} by comparing initial reaction rates at 298, 303, and 308 K. The occurrence of external diffusion limitation can thus be excluded.

The effects of solvents on rates and selectivity are complex, but some trends are nevertheless clear. First, stronger adsorption of the solvent results in decreased intraporous substrate concentrations and low rates. Preliminary sorption experiments show that toluene strongly adsorbs on $[Cu_3(btc)_2]$, in agreement with the low rates observed in toluene. Secondly, solvents with free electron pairs that specifically sorb on the Cu^{II} sites may block the active sites and hinder conversion of **1**; this probably explains the low rates found when acetonitrile is used. Finally, the results with methanol are likely to be influenced by the slightly Brønsted acid properties of the solvent itself, which may be enhanced by coordination of methanol on the Lewis acid sites: reaction rates are higher but selectivities are lower. The selectivity of **2** thus only reflects the Lewis acid properties of $[Cu_3(btc)_2]$ if appropriate solvents are used.

A series of reference reactions was carried out with known Lewis and Brønsted acids in the same solvents and conditions to compare the results with those obtained with $[Cu_3(btc)_2]$. Results are given in Table 4. The time to reach the indicated conversion is included as an estimation of reaction rate. Selected reference catalysts were, for example, known homogeneous catalysts ($CuCl_2$ and particularly $ZnBr_2$), contained weakly coordinating anions ($Cu(OTf)_2$ and $Cu(ClO_4)_2$), were the same Cu–carboxylate paddlewheel as $[Cu_3(btc)_2]$ ($CuAc_2$; Ac = acetate), showed microporosity (zeolite CuY), were synthetic precursors to $[Cu_3(btc)_2]$ ($Cu(NO_3)_2$ and H_3BTC), or showed Brønsted acidity (Amberlite IRC50, Dowex 50Wx4-100). Again solvents are expected to influence the reactivity of these catalysts, for example, by affecting the solubility or by coordinating to the Lewis acid. Selectivities with $[Cu_3(btc)_2]$ are significantly higher than the values for the reference catalysts, except for $ZnBr_2$ in toluene. However, reaction rates of $[Cu_3(btc)_2]$ are lower than those of the best Lewis acid catalysts. For reactions in DCE, it can be seen that, with the exception of $CuOAc_2$, all selectivities obtained with Lewis acids lie well above 50%, while this threshold is not crossed with the Brønsted acid catalysts, such as H_3BTC, the carboxylic resin Amberlite IRC-50, or the sulfonic resin Dowex 50Wx4-100. The selectivity obtained with CuY is comparable to that of the other Lewis acid materials. In ethyl acetate or toluene, the results are quite similar to those obtained in DCE: the Lewis acids catalyze the isomerization reaction with significantly higher selectivities than the Brønsted acids. Only methanol is an exception: the reaction even proceeds without a catalyst, and differences between Lewis and Brønsted acids are much less clear.

An interesting comparison can be made between the activities and selectivities of the synthetic precursors of $[Cu_3(btc)_2]$ versus $[Cu_3(btc)_2]$ itself. $Cu(NO_3)_2$ is very active but moderately selective, while H_3BTC is almost inactive. Surprisingly, $CuAc_2$ was almost inactive, though its low solubility may explain this behavior.

Cyclization of citronellal: The cyclization of citronellal was used as a second test reaction to monitor the acidity of a catalyst. This reaction shows a complex selectivity pattern, as each of its enantiomers can be converted to four different

Table 4. Conversions (*C*) of **1**, selectivities (*S*) for **2**, for Lewis and Brønsted acid reference catalysts. Reactions were carried out at 298 K with for each reaction 0.1 g of α-pinene oxide in 5 mL of solvent added to 0.1 g of catalyst.[a]

	DCE			EtOAc			MeOH			Toluene		
	S [%]	*C* [%]	*t* [h]	*S* [%]	*C* [%]	*t* [h]	*S* [%]	*C* [%]	*t* [h]	*S* [%]	*C* [%]	*t* [h]
$Cu(NO_3)_2$	65[b]	26	0.21	46[b]	100	0.07	31	98	0.5	n.d.	n.d.	n.d.
$CuAc_2$	44	5	55	–	0	56	–	0	7	n.d.	n.d.	n.d.
$CuCl_2$	65	66	53	40	83	56	24	100	1.5	n.d.	n.d.	n.d.
$Cu(OTf)_2$	75[b]	96	0.07	65[b]	100	0.18	n.d.	n.d.	n.d.	n.d.	n.d.	n.d.
$Cu(ClO_4)_2$	67[b]	100	0.03	43	100	2	n.d.	n.d.	n.d.	n.d.	n.d.	n.d.
$ZnBr_2$	67[b]	100	0.7	68	100	26	34	28	0.83	93	100	1
H_3BTC	44	3	71	–	0	49	n.d.	n.d.	n.d.	n.d.	n.d.	n.d.
Amberlite IRC-50	40	2	50	–	0	50	35	92	19	30	3	14
Dowex 50Wx4-100	46	45	50	27	98	50	0	100	1.5	40	100	20
zeolite CuY	64	11	25	68	4	26	75	15	40	n.d.	n.d.	n.d.
blank	22	4	238	–	0	238	30	80	25	–	0	73

[a] DCE = 1,2-dichloroethane; *S* = selectivity; *C* = conversion; *t* = time; n.d. = not determined; – = no conversion observed. [b] 1/3 of the standard amount of catalyst, because of a too fast reaction.

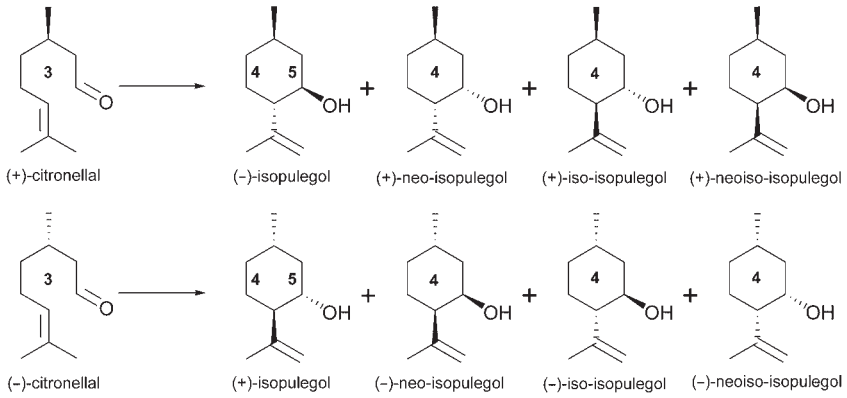

Scheme 2. Cyclization of racemic citronellal (**3**) to **4** and **5**.

cyclic products (Scheme 2). One of these products, (−)-isopulegol, is readily hydrogenated to the industrially important menthol.[25] We used racemic citronellal for our experiments, denoted as **3**. The eight product isomers are denoted together as **4**. From **4**, (+)-isopulegol and (−)-isopulegol are the most desired, and the two enantiomers are denoted together as **5**. With Lewis acids, high selectivities of **5** can be reached, especially when metal halogenides are used. With Brønsted acids, the ratio of **5** to **4** is usually significantly lower than with Lewis acids, but enantiomers **5** are still most abundant. Possible side reactions are subsequent etherification, cracking, or dehydration of **4**.[25–27]

Results of reactions at 383 K in toluene, DCE, and chlorobenzene (Table 5) show that no products other than **4** were formed when using $[Cu_3(btc)_2]$ obtained by means of different synthesis procedures or pretreatments. Again, selectivities remained constant till complete conversion, with a selectivity for **5** between 65 and 69%. To achieve high rates, DCE is a better solvent than aromatic solvents, reflecting that the latter have a higher sorption affinity for the microporous framework (Figure 9, top). Again, washing with EtOH, as in **Cu1d**, seriously decreases the rate (Figure 9, bottom). Crystal size has only a marginal effect on the rates. For the reactions in toluene, the activation energy was estimated to be 47 kJ mol^{-1} by comparing reaction rates at 378, 383, and 388 K.

Table 5. Selectivities *S* to **4** and **5** obtained with different $[Cu_3(btc)_2]$ catalyst samples in toluene. Reactions were carried out at 383 K with 0.5 g of citronellal in 5 mL of solvent added to 0.1 g of $[Cu_3(btc)_2]$.[a]

	Solvent	*S* for **4** [%]	*S* for **5** [%]
Cu1a	toluene	100	66
Cu1b	toluene	100	66
Cu1d	toluene	100	69
Cu1f	toluene	100	66
Cu2	toluene	100	65
Cu3	toluene	100	66
Cu1a	DCE	100	66
Cu1a	PhCl	100	68

[a] DCE = 1,2-dichloroethane. Selectivities remained constant until complete conversion.

Comparison with other Cu catalysts shows that $[Cu_3(btc)_2]$ displays similar or lower rates but selectivities that are at least comparable (Table 6). Only $ZnBr_2$ has clearly superior selectivity. With several catalysts, products other than **4** were formed, either because of bad initial selectivity ($CuAc_2$, $Cu(NO_3)_2$), or because of consecutive reactions at full conversion. When the isopulegol (**5**) fraction in the total of pulegols **4** is considered (**5**/**4**), again the distinction between Lewis and Brønsted acidity can be made. For carboxylic acids such as H_3BTC and Amberlite, the selectivity is appreciably lower than for the Cu Lewis acids.

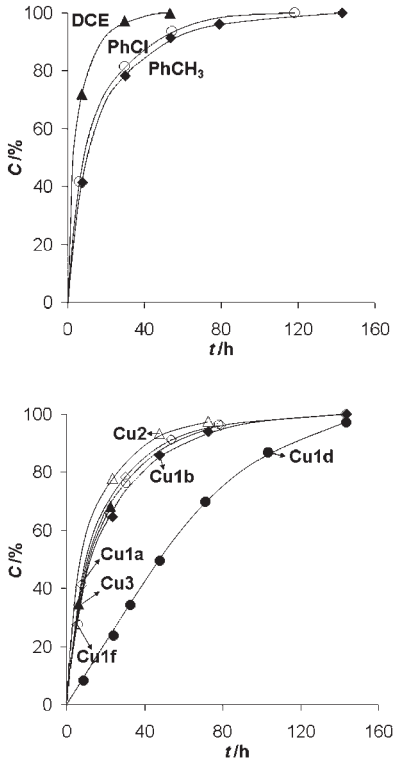

Figure 9. Conversion of **3** as a function of time. Top: in different solvents ($PhCH_3$ = toluene; DCE: 1,2-dichloroethane; PhCl = chlorobenzene). Bottom: for different pretreatments and synthesis procedures in toluene.

Heterogeneity and reusability of $[Cu_3(btc)_2]$: As a proof of the heterogeneous character of $[Cu_3(btc)_2]$, filtration tests were carried out for the reaction of **1** in DCE and **3** in toluene. It is clear from Figure 10 (top) that no leaching occurred in the reaction with **1**; no conversion was noticed with-

Table 6. Reaction of citronellal to **4** and **5** with Lewis and Brønsted acid reference catalysts in toluene. Reactions were carried out at 383 K with 0.5 g of citronellal in 5 mL of solvent added to 0.1 g of catalyst, unless indicated otherwise.[a]

Catalyst	*S* for **4** [%]	*S* for **5** [%]	**5**/**4** [%]	*C* [%]	*t* [h]
$Cu(NO_3)_2$	34	23	68	15	26
$CuAc_2$	63	45	71	19	142
$CuCl_2$	95	64	67	100	27
$Cu(OTf)_2$[b]	100	70	70	14	0.1
	10	7.7	77	100	7
$Cu(ClO_4)_2$[b]	100	69	69	5	0.3
	7	5	71	97	7
$ZnBr_2$[b]	100	94	94	100	27
H_3BTC[c]	100	48	48	3	26
Amberlite IRC-50	100	55	55	3	27
Dowex 50Wx4–100	52	34	65	100	0.2
Zeolite CuY	100	65	65	89	26
blank	100	74	74	12	164

[a] *S* = selectivity; *C* = conversion; *t* = time. [b] Reaction at 298 K because of fast reaction. [c] H_3BTC = benzene-1,3,5-tricarboxylic acid.

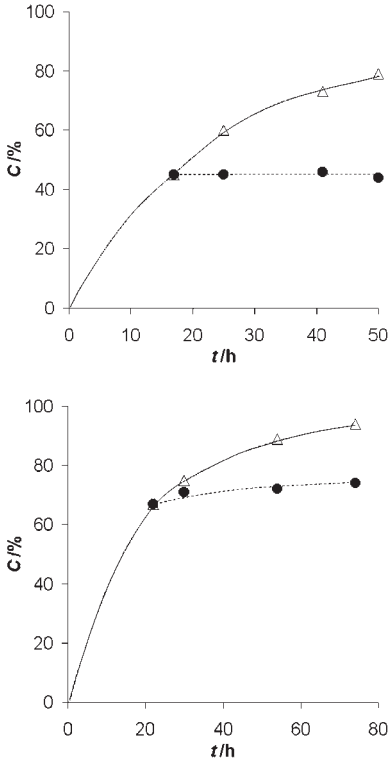

Figure 10. Filtration experiments for **1** (top) and **3** (bottom). Conversions are given as function of time. In both graphs, the full line represents the normal reaction with **Cu1a** as catalyst. The dashed line represents the reaction course after withdrawing the catalyst.

out catalyst. After removing the catalyst from a reaction mixture of **3**, conversion proceeded very slowly (Figure 10, bottom), but this is to be ascribed to the blank reaction of **3** occurring in toluene, which has a comparable rate (Table 6). No dissolved active species are thus assumed to be present in reaction mixtures with $[Cu_3(btc)_2]$. Regeneration experiments with **Cu1a** for reactions of **1** and **3** are described in the Experimental Section and are represented in Table 7. Selectivity and conversion were measured after each run. Selectivity remains constant after several reaction runs, but

Table 7. Regeneration experiments with **Cu1a** for reactions with **1** and **3**. After each reaction run, the catalyst sample was washed three times with the indicated solvent and allowed to dry. A double slash in the first column indicates an intermediate drying step (see Experimental Section).[a]

Reaction	Run	*S* [%]	*C* [%]	*t* [h]
1 in DCE	1	82	67	48
	2	82	19	48
1 in DCE	1	81	43	20
	2	81	19	20
	3	84	13	20
1 in DCE//ethanol/water	1	82	77	48
	2	78	60	48
3 in toluene	1	64	82	48
	2	65	26	48
3 in toluene//ethanol/water	1	65	76	48
	2	65	68	48

[a] Standard reaction conditions. *S* = selectivity; *C* = conversion, *t* = time.

reaction rate decreases for each consecutive run. For samples regenerated by washing in the reaction solvent, the decrease in activity was most severe. However, for samples regenerated by washing successively in ethanol, ethanol/water, and pure water after a first washing treatment in the reaction solvent, the activity could be restored almost to its initial value, especially for reactions in citronellal. The loss of activity might be partly attributed to a small loss of catalyst during successive washing treatments. It was noticed from light microscopy measurements that the catalyst crystals suffered from fragmentation during reactions. However, a comparison of X-ray diffraction patterns of **Cu1a** before and after several reaction runs did not reveal significant differences (Figure 11). A porosity measurement was carried out on the sample in the first entry of Table 7. A specific surface of 390 $m^2 g^{-1}$ and a pore volume of 0.153 $cm^3 g^{-1}$ were obtained. Comparing these values to those obtained from a freshly synthesized sample, the parallel decrease in pore

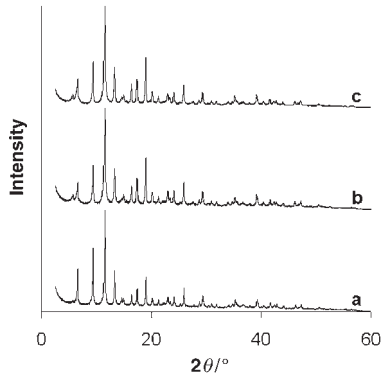

Figure 11. X-ray diffractograms of **Cu1a** after several reaction runs: directly after synthesis, as a reference (c), after two reactions runs of 48 h each with **1** (b), and after a reaction of 48 h with **3** (a).

volume and specific surface and in reaction rates over several runs can be attributed to formation of deposits inside the pores. The presence of deposits has been proven by IR measurements on samples after a 48 h reaction by the appearance of characteristic bands in the 2850–3000 cm^{-1} region of the spectrum. In parallel with the decrease of their activity, catalysts washed in the reaction solvents no longer switched colors from light blue to dark purple/blue upon drying; however, catalysts washed successively in ethanol, ethanol/water, and water still developed a clear purple shade after overnight drying.

Rearrangement of the ethylene acetal of 2-bromopropiophenone: A third test reaction, the rearrangement of the ethylene acetal of 2-bromopropiophenone (**6**), allowed us to obtain a more detailed view on the acid sites of a catalyst. This reaction was first developed in the search for new catalytic pathways to the synthesis of anti-inflammatory compounds like ibuprofen. It was found that the desired products, α-aryl propionic acids, could only be obtained with the specific group of hard Lewis acids, while soft Lewis acids and Brønsted acids produced other compounds.[28–31] The reaction pathways are summarized in Scheme 3. Our reaction

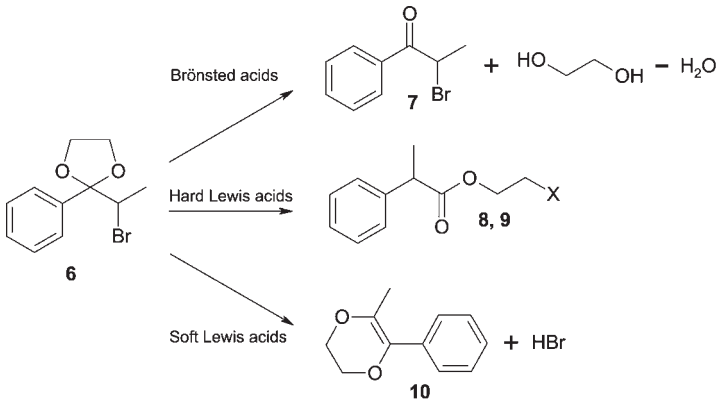

Scheme 3. Reaction of the ethylene ketal of 2-bromopropiophenone (**6**) to 2-bromopropiophenone (**7**), 2-bromoethyl 2-phenylpropanoate (**8**), 2-chloroethyl 2-phenylpropanoate (**9**) and 5-methyl-6-phenyl-2,3-dihydro-1,4-dioxin (**10**). X = Br (**8**) or Cl (**9**).

mixtures contained the following compounds: the Brønsted acid product 2-bromopropiophenone (**7**); 5-methyl-6-phenyl-2,3-dihydro-1,4-dioxin (**10**), the soft Lewis acid product; and 2-bromoethyl 2-phenylpropanoate (**8**) and 2-chloroethyl 2-phenylpropanoate (**9**), which are both hard Lewis acid products. Identification of the compounds **8** and **9** was difficult due to the low intensity of the characteristic bromine- and chlorine-containing parent ions in the mass spectra (see Experimental Section). The formation of **9** instead of **8** can be ascribed to halogen scrambling, for instance when chlorinated catalysts or solvents are used.[28] In more recent publications, 2-hydroxyethyl 2-phenylpropanoate has been proposed as well as the hard Lewis acid reaction product, while neither **8** or **9** were reported.[29–31] Perhaps small differences in reaction conditions, for instance in the amount of water present in the reaction mixture, may cause the formation of a hydroxyl- instead of a halogen-functionalized molecule. However, this does not change the assignment of the different products to the different acid sites, because ester formation is the crucial step in the reaction on a hard Lewis acid.

The results of the reactions with $[Cu_3(btc)_2]$ are given in Table 8. The selectivity of the esters (**8** + **9**) expresses the global selectivity to hard Lewis acid products. Compound **8**

Table 8. Selectivities *S* for the different products and conversions *C* in the reaction of **6** catalyzed by $[Cu_3(btc)_2]$. Reactions were carried out at reflux with catalyst and product amounts as in literature.[30,31]

	Solvent	*S* [%]					*C* [%]	*t* [h]
		7	**8**	**9**	**8+9**	**10**		
Cu1a	C_6H_5Cl	0	68	5	73	27	51	29
Cu2	C_6H_5Cl	0	80	2	83	17	13	22
Cu1a	$C_6H_4Cl_2$	0	73	2	75	25	81	1
		1	71	3	74	26	91	1
		1	66	6	72	27	97	2
		1	63	9	72	27	99	3
		1	56	15	70	29	100	5
Cu1a	C_6H_6	26	74	0	74	0	1	6
		17	72	0	72	11	3	23
		14	75	0	75	11	4	30

is clearly the major product in reactions with $[Cu_3(btc)_2]$ in chlorobenzene, which lead to the identification of $[Cu_3(btc)_2]$ as a hard Lewis acid.[30] Minor amounts of **9** were also formed, and traces of **7** are present in the reaction with **Cu1a**. With **Cu2**, the quantity of **8** is higher than with **Cu1a**. The product distribution is somewhat altered by using another procedure[31] in 1,2-dichlorobenzene as the reflux solvent: the reaction proceeds faster because of the higher reflux temperature and more **9** is formed. The time dependence of the selectivity for **9** suggests that **9** is formed from **8** by a secondary reaction. A silver nitrate test gave no evidence for free chloride impurities in the solvent; hence 1,2-dichlorobenzene itself is the likely source of Cl. In refluxing benzene, the reaction proceeded more slowly and, as expected, no **9** was detected at all.

Reference reactions with Lewis and Brønsted acids were carried out in chlorobenzene at reflux (Table 9). Solvent nitration was observed with $Cu(NO_3)_2$ as catalyst. With metal chlorides, compound **9** becomes the major product upon completion of the reaction, which illustrates the halogen scrambling when Cl sources are available. No **9** was formed with $ZnBr_2$. H_3BTC was not reactive at all, while Dowex 50Wx4-100 converted the acetal **6** back to the ketone **7**. On zeolite CuY, the Brønsted acid product initially prevails, but many side reactions were observed.

IR spectroscopy of adsorbed CO: Whereas infrared spectroscopy is commonly used for structural characterization of MOFs,[19] little work has been reported on the spectroscopic characterization of the surface properties of MOFs.[32] Pyri-

Table 9. Selectivities *S* to the different products obtained from **6** with a series of reference catalysts. Reactions were carried out in chlorobenzene with 0,1 g of **6** in 50 mL of chlorobenzene with 0.35 g of catalyst.

	S [%]					*C* [%]	*t* [h]
	7	**8**	**9**	**8+9**	**10**		
$Cu(NO_3)_2$	–	–	–	–	–	0	0.6
$CuCl_2$	8	17	75	92	0	5	8.3
	4	9	87	96	0	10	24
$ZnCl_2$	0.2	71	16	88	12	55	2.2
	0.2	60	27	87	13	85	5.3
	0.1	30	57	87	13	100	21.5
$ZnBr_2$	0	92	0	92	8	17	0.8
	0	87	0	87	13	65	5.8
H_3BTC	–	–	–	–	–	0	43
Dowex 50Wx4–100	100	0	0	0	0	3	2.8
	100	0	0	0	0	6	23.8
zeolite CuY[a]	86	1	2	3	0	91	1.8
	72	1	4	5	2	96	4.9
	34	1	10	11	1	100	24.0

[a] Other side products were formed.

dine can generally not be used as a probe molecule for MOFs with aromatic ligands, because of the coincidence of the absorption lines of pyridine and the substituted aromatic compounds (Figure 12). Carbon monoxide is a more suitable

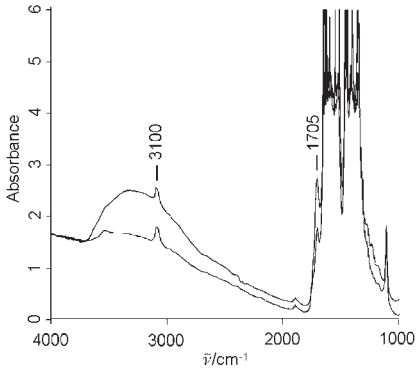

Figure 12. IR spectra before and after activation of **Cu1a** at 423 K.

probe, because of the window between 2500 and 2000 cm^{-1} in the spectra of $[Cu_3(btc)_2]$. A weak band in the carbonyl region at 1705 cm^{-1} may point to a very small amount of free carboxylic groups, but the narrow and intense ν(OH) band expected for an isolated Brønsted acid, benzenetricarboxylic acid, is not observed, confirming that the amount of uncomplexed BTC in the solid is small.

Figure 13 shows the spectra recorded on $[Cu_3(btc)_2]$ during progressive adsorption of CO at 100 K. The ν(CO) vibration bands are observed, but they are not linked to any perturbation of the spectrum in the ν(OH) region (not shown). Clearly, CO does not establish hydrogen bonds with the surface; there are indeed no Brønsted sites on the material. Bands appearing between 2200 and 2100 cm^{-1} are due to ν(CO) vibrations of CO interacting with Lewis sites. The initial ν(CO) vibration at 2123 cm^{-1} observed at low CO coverage is due to interaction with Cu^I cations, as the 3d

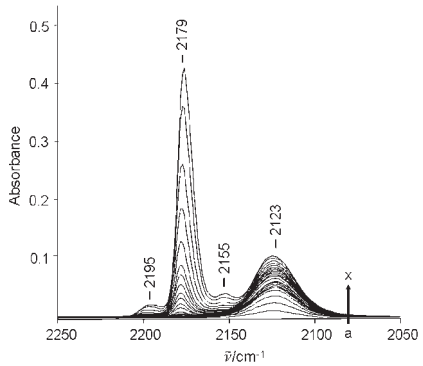

Figure 13. IR spectra of adsorbed CO on **Cu1a**.

electron transfer to the CO π^* orbital is more efficient for Cu^I.[33] The more intense ν(CO) band at 2179 cm^{-1} observed at higher coverage is due to CO interacting with Cu^{II} centers, and the low intensity bands at approximately 2155 and 2195 cm^{-1} arise from the formation of polycarbonyl species. Lewis sites are thus detected in large amounts, but the exact determination of the Cu^I/Cu^{II} ratio is impossible, because of the preferred interaction of CO with Cu^I. Saturation of the 2179 cm^{-1} band was never reached because of the very high amount of Cu^{II} in the solid. It should be noted that part of the Cu^I may be formed from Cu^{II} during the CO adsorption; similar reductions have been previously observed.[34]

Discussion

The synthesis and washing procedures that were developed in the present work lead to an X-ray pure structure with high specific surface area and pore volume. The three catalytic test reactions allowed us to obtain a clear picture of the catalytic activity of the acid sites in $[Cu_3(btc)_2]$. The isomerizations of α-pinene oxide and citronellal clearly identify $[Cu_3(btc)_2]$ as a Lewis acid, if the right solvents and appropriate reference catalysts are used. In the more refined test with **6**, $[Cu_3(btc)_2]$ was identified as a hard Lewis acid. In the comparison between $[Cu_3(btc)_2]$ and its synthetic precursors, it was shown that its two synthetic precursors, each unsuitable catalysts, were combined in $[Cu_3(btc)_2]$ to obtain a good catalyst. The organic ligand, H_3BTC, had generally a low activity in the isomerization reactions. There is no evidence that protonated benzenetricarboxylic acid, for example, at the surface of $[Cu_3(btc)_2]$ or at defects in its structure, would significantly contribute to the overall acid activity. When $[Cu_3(btc)_2]$ is compared with its precursor $Cu(NO_3)_2$, it is seen that the activity of the Cu^{II} decreases, but its selectivity increases by its incorporation in BTC complexes.

The results of the catalytic tests are in fair agreement with the IR spectroscopic study. The large amount of Lewis sites present and the absence of Brønsted sites in the solid were confirmed in these experiments. Some Cu^I cations were detected in low quantity, and these probably correspond to the Cu_2O oxide particles observed in visual microscopy. Howev-

er, the large majority of the Cu is in the divalent state, as was also proven by XPS.

Different synthesis procedures did not seem to influence the catalytic results much. Experiments with different crystal sizes, as well as experimentally determined activation energies, indicate that reagent diffusion is not limiting the reaction rates, at least for the reactions of the present study. Regarding the washing treatments, we reason that at least one washing step in ethanol/water (50:50) should be included because unreacted H_3BTC dissolves quite poorly in pure water. Excessive exposure to water degrades the structure, but in practice this poses no real problem, as long as one performs reactions in common organic solvents. These solvents do not have to be dried, nor is exposure of the structure to atmospheric moisture noxious. Filtration and regeneration experiments show that the activity of $[Cu_3(btc)_2]$ decreases because of the formation of deposits in the pores. Particularly for the isomerization of **1** this is not surprising, since **1** is a very reactive and rather large molecule.[24,35] However, by using regeneration procedures with ethanol and water as solvents, catalytic activities could be brought back close to their original values.

In conclusion, the well-defined Lewis acid sites and the high selectivities observed for several important isomerization reactions on $[Cu_3(btc)_2]$ are a strong incentive for further exploration of MOFs as catalysts. While the activity and the resistance towards deactivation are amenable to improvement, there is no doubt that the current flood of new MOF structures will result in several catalytic materials of high interest.

Experimental Section

Instrumentation: Light microscopic images were obtained with a Jenaval light microscope with amplifications of 10 and 25 coupled to a JVC TK-C1381 color video camera. SEM measurements were conducted on a Philips SEM XL30 FEG. XRD patterns were measured on a STOE StadiP operating in high-throughput mode using $Cu_{K\alpha}$ radiation with a wavelength of 1.5418 Å. Measurements were carried out between 2θ values of 2.5 and 60° with a step of 300 s (1 step: 1.5°). Nitrogen physisorption measurements were carried out on a Coulter Omnisorp 100 CX and analyzed with the program Coulter SA-Reports. Before measurement, each sample was heated overnight at 423 K in vacuum. TGA measurements were carried out on a TGA Q500 of TA instruments operating in high-throughput mode. Surface XPS measurements were conducted with a Perkin–Elmer PHI ESCA 5500 system equipped with a monochromatic $Al_{K\alpha}$ source. The base pressure of its analysis chamber was below 1×10^{-7} Pa. Experiments were performed with 220 W source power and an acceptance angle of about 7°. The analyser axis made an angle of 45° with the sample surface. A general survey with a binding energy range of 0–1400 eV at pass energy 187.85 eV was recorded. Next, the C1s, O1s, Cu2p and 3p core levels were measured in high-resolution mode (pass energy 58.70 eV, step 0.13 eV). Gas chromatographic analyses were performed on a HP 6850 Agilent GC with automatic injection system, a capillary HP-1 column and an FID detector. The chosen temperature program allowed baseline separation of all compounds. GC-MS measurements were performed on an Agilent 6890 GC with HP-5MS column, coupled to an Agilent 5973 Network MSD mass spectrometer. Infrared spectra were recorded using a Bruker s66 spectrometer, operated at 4 cm^{-1} optical resolution and four levels zero-filling, on self supporting wafers (2 cm^2, ca. 15 mg) of the solid, prepared by application of a pressure of 5×10^7 Pa. The wafers were placed into a vacuum infrared quartz cell. The cell allowed for heating of the sample for pretreatment and cooling to 100 K in the infrared beam, as well as introducing known quantities of gas into the cell. The wafers were activated under vacuum by heating during 2 h from 298 K to 423 K, then dwelling at that temperature for 2 h. The cell was cooled by liquid nitrogen so that the sample reaches the temperature of 100 K, and CO was introduced progressively into the cell in steps of ca. 0.1 μmol.

Synthesis of catalysts: An appropriate synthesis procedure for $[Cu_3(btc)_2]$ was first sought in order to obtain a pure sample with small crystals. The procedure of Schlichte et al., developed in a catalytic context, was chosen from different reported synthesis procedures.[2,7,13] This procedure was slightly adapted by lowering the synthesis temperature to avoid the formation of Cu_2O from Cu^{II}. Briefly, a solution of $Cu(NO_3)_2{\cdot}3H_2O$ (4.86 g; p.a., Fluka) in doubly distilled water (66.67 g) was stirred with a solution of H_3BTC (benzene-1,3,5-tricarboxylic acid (trimesic acid); 2.33 g; 98%, Acros) in pure ethanol (52.00 g; 100%, Normapur) for 30 min and then divided into four teflon-lined steel autoclaves with a volume of 33 mL each. After 15 h at 383 K, the autoclaves were immediately cooled down to room temperature. The pale green supernatant contained unreacted $Cu(NO_3)_2$ and H_3BTC, together with HNO_3 as is evident from the stoichiometry of the synthesis reaction [Eq. (1)].

$$3\,Cu(NO_3)_2 + 2\,H_3BTC + 3\,H_2O \rightarrow [Cu_3(btc)_2]\cdot 3\,H_2O + 6\,HNO_3 \qquad (1)$$

To eliminate Brønsted and Lewis acids other than the MOF structure itself, different washing procedures were tried out (Table 9). The content of one autoclave was washed with 200 mL of solvent for each washing step. Catalysts **Cu1a** were washed twice quickly (30 s) with a mixture of ethanol/water (50:50) and subsequently quickly washed three times with doubly distilled water. Catalysts **Cu1b** were three times quickly washed in doubly distilled water. Catalysts **Cu1c** were vigorously stirred three times in doubly distilled water over periods of 10 min each. Care should be taken when treating $[Cu_3(btc)_2]$ with excess water: when the material was stirred in water for more than 3 h, a disintegration of the structure was observed. Catalysts **Cu1d** were quickly washed three times in pure ethanol (100%, Normapur). Catalysts **Cu1e** were quickly washed three times in an ethanol:water (50:50) mixture. More drastic washing procedures with triethylamine (99%, Acros) or a saturated solution of $NaHCO_3$ (p.a., Acros) resulted in a quick or immediate dissolution of $[Cu_3(btc)_2]$, respectively. Catalysts **Cu1a–e** were first dried at 333 K for 4 h and then overnight at 383 K. To see an influence of drying temperature, catalysts **Cu1f** were dried overnight at 473 K. The color of **Cu1f** was deeper blue and less violet than the color of all other samples. Larger crystals (**Cu2**) were obtained by another literature procedure, in which the temperature was also decreased to 383 K.[7] A third procedure (**Cu3**) was identical to that followed for **Cu1a**, but with half the reagent concentrations used; it resulted in slightly smaller $[Cu_3(btc)_2]$ crystals.

Zeolite CuY was prepared by using zeolite NaY (FAU) from Zeocat with a Si/Al ratio of 2.7 following a literature procedure.[36] After exchange, the zeolites were dried in air at 383 K. Next, the catalyst was calcined during 5 h at 723 K with a ramping rate of 1 K min^{-1}. The final amount of Cu was determined at 11 wt% with ICP. All other catalysts were used as received: $Cu(NO_3)_2{\cdot}3H_2O$ (p.a., Acros), $CuAc_2$ (99%, Acros), $CuCl_2$ anhydrous (99%, Acros), $Cu(OTf)_2$ (99%, AlfaAesar), $Cu(ClO_4){\cdot}6H_2O$ (98%, Acros), $ZnBr_2$ (98%, Fluka), $ZnCl_2$ (99%, Aldrich), H_3BTC (98%, Acros), Amberlite IRC50 (Acros) and Dowex 50Wx4-100 (Aldrich).

Catalytic reactions: α-pinene oxide (97%, Acros) and citronellal (citronellal pract., 93%, Acros) were commercially obtained. The ethylene acetal of 2-bromopropiophenone (97%, Aldrich) was prepared according to a literature procedure with a purity of 99%.[30] Solvents were dry and of the highest grade available: 1,2-dichloroethane (99%, GPR), ethyl acetate (p.a., Acros), methanol (p.a., ChemLab), toluene (HPLC grade, Fisher), acetonitrile (HPLC grade, Acros), benzene (p.a., UCB), chlorobenzene (99+%, Acros), 1,2-dichlorobenzene (99%, Acros). Before conducting reactions, the compatibility of $[Cu_3(btc)_2]$ with the solvents

was checked. After stirring for 72 h at room temperature in the various solvents, no differences were noticed in the X-ray diffractograms. Before reaction, a freshly prepared catalyst sample was dried overnight at 383 K. The reference Lewis acid catalysts and H_3BTC were stirred in the appropriate solvent over a 72 h period to ensure maximum solubility. Depending on the solubility of these reference catalysts, reactions were partly or totally homogeneous or heterogeneous. The ion exchange resins were dried overnight at 333 K before reaction. For the reactions with α-pinene oxide, 0.1 g was added to 0.1 g catalyst with 5 mL of solvent. Reactions were carried out at 298 K. For the reactions with citronellal, 0.5 g was added to 0.1 g catalyst with 5 mL of solvent. Reactions were carried out at 383 K. For the filtration tests, part of the reaction suspension was withdrawn at a certain conversion at reaction temperature, the catalyst was separated, and the supernatant was allowed to react further in a separate vial. Regeneration tests were identical to the normal reactions; after reaction, the catalyst was quickly washed three times in the same solvent as used in the reaction, dried at 333 K and subsequently overnight at 383 K before the next run. Hereafter, as a second regeneration procedure, a number of samples was successively washed in ethanol, ethanol/water and twice in water and finally dried in two steps. For the reactions with the ethylene acetal of 2-bromopropiophenone, two literature procedures were followed with chlorobenzene or 1,2-dichlorobenzene as reflux solvents.[30,31] The samples were immediately analyzed with GC or GC-MS. GC-MS data for **7** were *m*/*z* (%): 258 (3) [M^+(^{81}Br)], 256 (3) [M^+(^{79}Br)], 150 (2), 133 (1), 105 (100), 79 (7), 77 (10), 51 (4); for **8**: 214 (1) [M^+(^{37}Cl)], 212 (3) [M^+(^{35}Cl)], 150 (1), 133 (3), 105 (100), 79 (7), 77 (9), 51 (4); for **9**: 176 (33) [M^+], 115 (5), 105 (100), 77 (38), 51 (10).

Acknowledgement

The authors are grateful to H. Leeman for SEM measurements and to G. Vanbutsele for nitrogen physisorption measurements. LA wishes to thank F.W.O. (Research Foundation Flanders) for financial support. DDV is grateful to F.W.O. for grant G.0323.04. This work was performed in the frame of the Belgian Interuniversity Poles of Attraction (IUAP V-3).

[1] H. Li, M. Eddaoudi, M. O'Keeffe, O. Yaghi, *Nature* **1999**, *402*, 276–279.
[2] S. Chui, S. Lo, J. Charmant, A. Orpen, I. Williams, *Science* **1999**, *283*, 1148–1150.
[3] J. Rowsell, O. Yaghi, *Microporous Mesoporous Mater.* **2004**, *73*, 3–14.
[4] S. Kitagawa, R. Kitaura, S. Noro, *Angew. Chem.* **2004**, *116*, 2388–2430; *Angew. Chem. Int. Ed.* **2004**, *43*, 2334–2375.
[5] C. Janiak, *Dalton Trans.* **2003**, 2781–2804.
[6] J. Lee, J. Li, J. , Jagiello, *J. Solid State Chem.* **2005**, *178*, 2527–2532.
[7] Q. Wang, D. Shen, M. Bülow, M. Lau, S. Deng, F. Fitch, N. Lemcoff, J. Semanscin, *Microporous Mesoporous Mater.* **2002**, *55*, 217–230.
[8] J. Rowsell, A. Millward, K. Park, O. Yaghi, *J. Am. Chem. Soc.* **2004**, *126*, 5666–5667.
[9] M. Eddaoudi, J. Kim, N. Rosi, D. Vodak, J. Wachter, M. O'Keeffe, O. Yaghi, *Science* **2002**, *295*, 469–472.
[10] U. Müller, M. Schubert, F. Teich, H. Puetter, K. Schierle-Arndt, J. Pastré, *J. Mater. Chem.* **2006**, *16*, 626–636.
[11] H. Dathe, E. Peringer, V. Roberts, A. Jentys, J. Lercher, *C. R. Chim.* **2005**, *8*, 753–763.
[12] B. Gómez-Lor, E. Guttiérez-Puebla, M. Iglesias, M. Monge, C. Ruiz-Valero, N. Snejko, *Chem. Mater.* **2005**, *17*, 2568–2573.
[13] K. Schlichte, T. Kratzke, S. Kaskel, *Microporous Mesoporous Mater.* **2004**, *73*, 81–88.
[14] C. Wu, A. Hu, L. Zhang, W. Lin, *J. Am. Chem. Soc.* **2005**, *127*, 8940–8941.
[15] L. Huang, H. Wang, J. Chen, Z. Wang, J. Sun, D. Zhao, Y. Yan, *Microporous Mesoporous Mater.* **2003**, *58*, 105–114.
[16] C. Lin, S. Chui, S. Lo, F. Shek, M. Wu, K. Suwinska, J. Lipkowski, I. Williams, *Chem. Commun.* **2002**, 1642–1643.
[17] T. Reineke, M. Eddaoudi, M. O'Keeffe, O. Yaghi, *Angew. Chem.* **1999**, *111*, 2712–2716; *Angew. Chem. Int. Ed.* **1999**, *38*, 2590–2594.
[18] M. Rosseinsky, *Microporous Mesoporous Mater.* **2004**, *73*, 15–30.
[19] O. Yaghi, C. Davis, G. , Li, H. Li, *J. Am. Chem. Soc.* **1997**, *119*, 2861–2868.
[20] L. Yang, H. Naruke, T. Yamase, *Inorg. Chem. Commun.* **2003**, *6*, 1020–1024.
[21] A. Corma, H. García, *Chem. Rev.* **2003**, *103*, 4307–4365.
[22] K. Wilson, A. Rénson, J. Clark, *Catal. Lett.* **1999**, *61*, 51–55.
[23] J. Kaminska, M. Schwegler, A. Hoefnagel, H. van Bekkum, *Recl. Trav. Chim. Pays-Bas* **1992**, *111*, 432–437.
[24] P. Kunkeler, J. van der Waal, J. Bremmer, B. Zuurdeeg, R. Downing, H. van Bekkum, *Catal. Lett.* **1998**, *53*, 135–138.
[25] C. Milone, C. Gangemi, G. Neri, A. Pistone, S. Galvagno, *Appl. Catal. A* **2000**, *199*, 239–244.
[26] C. Milone, A. Perri, A. Pistone, G. Neri, S. Galvagno, *Appl. Catal. A* **2002**, *233*, 151–157.
[27] P. Kropp, W. Breton, S. Craif, S. Crawford, W. Durland, J. Jones, J. Raleigh, *J. Org. Chem.* **1995**, *60*, 4146–4152.
[28] G. Castaldi, A. Belli, F. Uggeri, C. Giordano, *J. Org. Chem.* **1983**, *48*, 4658–4661.
[29] M. Baldoví, A. Corma, V. Fornés, H. García, A. Martínez, J. Primo, *J. Chem. Soc. Chem. Commun.* **1992**, 949–951.
[30] F. Algarra, A. Corma, V. Fornés, H. García, A. Martínez, J. Primo, *Stud. Surf. Sci. Catal.* **1993**, *78*, 653–660.
[31] A. Corma, H. García, A. Primo, A. Domenech, *New J. Chem.* **2004**, *28*, 361–365.
[32] A. Vimont, J. Goupil, J. Lavalley, M. Daturi, S. Surblé, C. Serre, G. Ferey, *J. Am. Chem. Soc.* **2006**, *128*, 3218–3227.
[33] K. Hadjiivanov, G. , Vayssilov, *Adv. Catal.* **2002**, *47*, 307–511.
[34] K. Hadjiivanov, H. Knözinger, A. Milushev, *Catal. Commun.* **2002**, *3*, 37–44.
[35] P. Mäki-Arvela, N. Kumar, V. Nieminen, S. Sjöholm, T. Salmi, D. Murzin, *J. Catal.* **2004**, *225*, 155–169.
[36] P. Smeets, M. Groothaert, R. Schoonheydt, *Catal. Today* **2005**, *110*, 303–309.

Received: February 16, 2006
Published online: ■■ ■■, 2006

Heterogeneous Catalysis

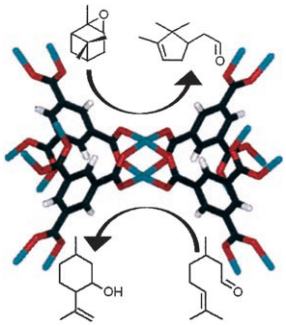

A systematic study of the catalytic properties of a metal-organic framework: $[Cu_3(btc)_2]$ is a very selective catalyst for specific isomerizations of terpenes, terpene epoxides, and ketals (see scheme). Together with IR spectroscopic measurements on adsorbed probe molecules, this proves the hard Lewis acid properties of the material.